


## RESEARCH ARTICLE

# A homogenization-based state-dependent model for gap-graded granular materials with fine-dominated structure

X. S. Shi<sup>1</sup>  | Jidong Zhao<sup>2</sup>  | Yufeng Gao<sup>1</sup> 

<sup>1</sup> Key Lab of Ministry of Education for Geomechanics and Embankment Engineering, Hohai University, Nanjing, China

<sup>2</sup> Department of Civil and Environmental Engineering, The Hong Kong University of Science and Technology, Kowloon, Hong Kong

## Correspondence

Xiusong Shi, Key Lab of Ministry of Education for Geomechanics and Embankment Engineering, Hohai University, Nanjing, 210098, China.

## Funding information

National Natural Science Foundation of China, Grant/Award Numbers: 51679207, 51908193; Fundamental Research Funds for the Central Universities, Grant/Award Number: B200201050; Research Grants Council of Hong Kong, Grant/Award Numbers: RGC/GRF Grant no. 16201419, TBRG Grant no. T22-603/15N, CRF Grant no. C6012-15G

## Abstract

Gap-graded granular soils are common natural soils composed of cohesionless granular matrix and rock aggregates. Since they are widely used as construction materials worldwide, their deformation behavior is crucial for the design of civil infrastructures. There have been rare constitutive models reported for gap-graded granular soils in the literature. This study presents a homogenization-based state-dependent model within the elastoplastic framework. The model features a homogenization equation with a structure parameter and a novel state-dependent dilatancy function to describe the behavior of granular matrix. Simulations of the model reveals that the initial stiffness and peak shear strength of gap-graded soils rely on both the coarse fraction and the initial density of granular matrix. The structure parameter is related to the internal structure of gap-graded soils, and it varies with the particle shape, and particle size distribution of rock aggregates. A higher value of the structure parameter indicates a more distinct coarse fraction effect of rock aggregates, that is, higher initial stiffness, higher peak shear strength, and higher residual shear strength. For a given coarse fraction, the critical states can be well fitted by a straight line through the origin, and the critical state strength parameter  $M_m$  increases with the rising rock fraction. A practical method is further proposed for the critical state line of gap-graded granular soils in  $e-p'$  compression plane. The proposed model is validated by using experimental data from the literature, including the soils with various densities of sand matrix, different particle size, and particle size distribution of rock aggregates. Comparison between measured data and model predictions indicates that the proposed model can well reproduce the stress-strain relationship and volumetric deformation behavior of sand-gravel mixtures and soil-rock mixtures.

## KEYWORDS

coarse fraction effect, elastoplastic model, gap-graded granular soils, homogenization, initial density of matrix

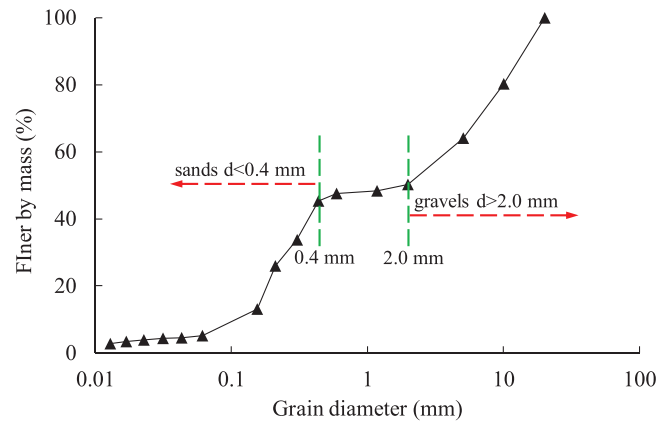


FIGURE 1 Typical particle size distribution of gap-graded granular materials (data cited from Chen et al., 2019a)

## 1 | INTRODUCTION

Gap-graded granular materials consist of granular particles, in which a range of particle size is missing. Figure 1 shows a particle size distribution curve of a natural residual soil from Western China.<sup>1</sup> The soil is a typical gap-graded granular material which is composed of small sand particles and large gravels. The sand particles in gap-graded soils are typically created due to the degradation of rock blocks during the change of weather factors, for example, seasonal moist change and temperature oscillation.<sup>2–5</sup> The gap-graded granular soils can also be created during transportation and further deposition process.<sup>6–9</sup> Gap-graded soils are usually treated as inhomogeneous materials, with the fines and voids being matrix and the aggregates being inclusions.<sup>10–12</sup> This type of soils are widely distributed in mountainous regions and are commonly used as construction and building materials.<sup>2,13</sup> The physical and mechanical properties of the gap-graded soils are affected by the presence of rock aggregates, especially when there are partial contacts between the aggregates.

It is well recognized that the mechanical behavior of gap-graded soils is associated with the coarse fraction: the behavior is dominated by fines with a fine fraction beyond the “transitional fine content,” and transients to be controlled by the coarse grain structure at a lower fine fraction.<sup>2,14,15</sup> In weathered residual soils, strong weathering induces fine-dominated structure where the coarse aggregates are floating in the fine matrix.<sup>1,16</sup> To this end, gap-graded soils with fine-dominated structure will be investigated in this work. The inclusions are usually randomly distributed in the fine matrix during weathering process.<sup>17,18</sup> In this case, the mechanical properties rely on the natural of coarse particles, coarse fraction and the properties of fine matrix, and the change of internal structure makes the nonuniformity and nonlinearity in terms of mechanical and physical properties.

Although substantial laboratory and numerical works on gap-graded granular soils are reported,<sup>3,13,19–22</sup> qualitative analyses and characterizations have been dominant, and theoretical work is relatively scarce. Shi et al.<sup>16</sup> proposed an elasto-plastic model for sand-clay mixtures within mixture theory. However, the model is not suitable for the gap-graded granular mixtures due to the following reasons: (1) the initial void ratio of granular matrix changes after being mixed with rock aggregates, and the initial state of matrix is related to the coarse fraction<sup>15,19,21,23</sup>; (2) the mechanical behavior relies on the initial state of matrix,<sup>24–26</sup> this state-dependent behavior distinguishes it from the sand-clay mixtures; (3) The interaction between the fine particles and the rock aggregates is based on discrete contacts, hence the homogenization law should be different from that of sand-clay mixtures.

It is well reported that the coarse fraction effect is affected by the stress level, the initial density of the fine matrix, and the nature of rock aggregates.<sup>2,16,27–29</sup> To evaluate the coarse fraction effect on the mechanical behavior of gap-graded granular soils, a new homogenization equation is adopted to correlate the overall tangent stiffness and the tangent stiffness of matrix. The homogenization equation is then incorporated into the elasto-plastic framework, and the model is further validated based on the data of drained triaxial compression tests from the literature.

## 2 | VOLUME-AVERAGE APPROACH

The gap-graded granular materials are a mixture of fine particles and rock aggregates. Since the fine content is higher than the “transitional fine content,” a composite soil arises without a significant proportion of macro-voids between coarse

aggregates. In this case, the structure of gap-graded soils (both in artificial or natural systems) may be assumed to be isotropic in a statistical point of view. As noted in previous studies,<sup>30–32</sup> this type of composites has isotropic macroscopic mechanical properties. Following the theory of elastoplasticity, the incremental strain is composed of an elastic part and a plastic part:

$$d\varepsilon_{ij} = d\varepsilon_{ij}^e + d\varepsilon_{ij}^p \quad (1a)$$

$$d\varepsilon_{ijm} = d\varepsilon_{ijm}^e + d\varepsilon_{ijm}^p \quad (1b)$$

where  $\varepsilon_{ij}$  and  $\varepsilon_{ijm}$  are the overall strain tensor of gap-graded soils and the strain tensor of fine granular matrix, respectively;  $d\varepsilon_{ij}^e$  ( $d\varepsilon_{ijm}^e$ ) and  $d\varepsilon_{ij}^p$  ( $d\varepsilon_{ijm}^p$ ) are the corresponding elastic and plastic parts. As noted by Shi and Yin,<sup>11</sup> the traditional mixture theory and volume average scheme can be also applied to gap-graded soils. In this kind of mixture system, the stiffnesses of the 2 phases are distinctly different, as well as the yield stress and work-hardening characteristics.<sup>33,34</sup> The deformation is concentrated within the matrix due to the incompressible rock inclusions. Applying volume-average scheme to the strains,<sup>18,33</sup> the overall strains of gap-graded soils is approximated by the values of matrix:

$$\varepsilon_{ij}^e = (1 - \phi_a)\varepsilon_{ijm}^e \quad (2a)$$

$$\varepsilon_{ij}^p = (1 - \phi_a)\varepsilon_{ijm}^p \quad (2b)$$

$$\varepsilon_{ij} = (1 - \phi_a)\varepsilon_{ijm} \quad (2c)$$

where  $\phi_a$  is the volume fraction of the rock aggregates, which is equivalent to the inter-granular void ratio.<sup>14</sup> Note that, in Equation (2), the rock aggregates are assumed to be incompressible compared with the soft matrix. Hence, the volume fraction of aggregates varies during the loading (unloading) process, and uniquely depends on the overall void ratio of gap-graded granular soils<sup>11</sup>:

$$\phi_a = \frac{\rho_m - \rho + \rho\psi_a}{(1 + e)\rho_m} \quad (3)$$

where  $e$  is the overall void ratio of a gap-graded soil;  $\psi_a$  is the coarse fraction, defined as ratio of mass of rock aggregates to the overall mass of gap-graded soils;  $\rho$  is the overall particle density:

$$\rho = \frac{\rho_m\rho_a}{\psi_a\rho_m + (1 - \psi_a)\rho_a} \quad (4)$$

where  $\rho_m$  and  $\rho_a$  are the particle density of fines and rock aggregates, respectively.

Both the matrix-bridges and the partial contacts between the aggregates induce nonuniform stress distribution in gap-graded soils.<sup>11,18,27</sup> Analogous to the definition of strain variables, the stress variables are defined using volume average approach. The overall stress tensor can be expressed in terms of the values of its 2 phases:

$$\sigma'_{ij} = (1 - \phi_a)\sigma'_{ijm} + \phi_a\sigma'_{ija} \quad (5)$$

where  $\sigma'_{ijm}$  and  $\sigma'_{ija}$  are the stress tensor of the matrix and rock aggregates, respectively. As noted by González et al.,<sup>34</sup> the above stress and strain variables can be well defined based on the concept of representative volume element (RVE). It is widely adopted in analyzing the behavior of multi-phase materials.<sup>18,34,35</sup>

### 3 | HOMOGENIZATION EQUATION FOR ELASTIC SHEAR STIFFNESS

The structure of gap-graded granular soils resembles that of the particle-reinforced materials, where the aggregates are randomly dispersed in the work-hardening matrix.<sup>33,36</sup> The traditional particle-reinforced theory assumes that the matrix

TABLE 1 Parameters for the estimation of structure variables

Sources	González-Hurtado and Newson (2015)	Ruan et al. (2018)
$\Xi$	0.64	1.35
$H$	0.74	0.60

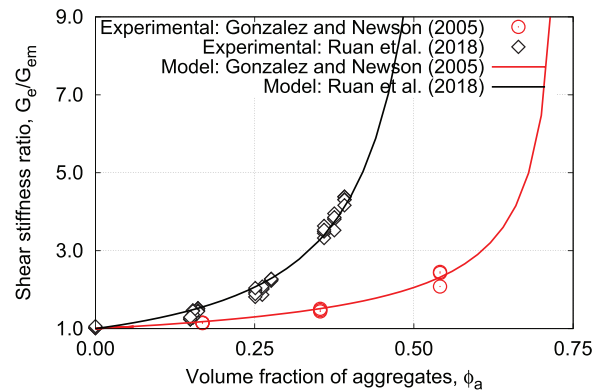


FIGURE 2 Relationship between structure parameter and volume fraction of coarse aggregates

and inclusions are perfectly bonded at the interface, without void growth or nucleation. However, since both fine particles and rock aggregates are cohesionless materials, the fines and the rock aggregates interact through discrete contacts with no bonding at the interface. The mechanisms governing the deformation behavior of gap-graded granular mixtures are different from that of traditional particulate-reinforced materials. The reinforcing effect of aggregates in granular mixtures relies mainly on partial contacts and densified matrix-bridges between adjacent aggregates.<sup>11,18,27,37,38</sup> Therefore, classical homogenization theory is not suitable for the deformation behavior of granular mixtures. To this end, a semi-empirical homogenization equation is proposed by Shi et al.<sup>18</sup> for the elastic shear stiffness of gap-graded granular materials based on DEM simulations:

$$\log G_e = \log G_{em} + \xi \log \left( \frac{\bar{\phi}_a}{\bar{\phi}_a - \phi_a} \right) \quad (6)$$

where  $G_e$  and  $G_{em}$  are the overall elastic shear stiffness and the elastic shear stiffness of matrix, respectively;  $\xi$  denotes a structure parameter controlling the effect of coarse fraction on the overall elastic shear stiffness of gap-graded granular materials. It is affected by the nature (shape and texture of aggregates) and the particle size distribution of aggregates. As noted by Shi et al.,<sup>18</sup> the influence of initial state, stress level and coarse fraction is negligible. Note that,  $\xi$  will not remain constant if particle breakage of aggregates occurs at high stress levels;  $\bar{\phi}_a$  is a model parameter related to the nature of rock aggregates. It corresponds to the densest packing state of gap-graded materials when the rock aggregate approaches its maximum packing density  $\bar{\phi}_a$ :

$$\bar{\phi}_a = \frac{1}{1 + e_{\min}^a} \quad (7)$$

where  $e_{\min}^a$  is the minimum void ratio of the rock aggregates.

The homogenization equation in Equation (6) reveals that the overall elastic shear stiffness is uncorrelated to the elastic shear stiffness of rock aggregates. This is different from the homogenization equations in classical homogenization theory<sup>39–41</sup> and that for lumpy soils.<sup>17</sup> The homogenization equation has been validated using the data from the literature, including (1) a mixture of silica sand and glass beads, with the sand and beads being the matrix and inclusion, respectively,<sup>42</sup> and (2) a sandy soil reported by Ruan et al.<sup>43</sup> The influence of stress levels, coarse fractions, and relative density are considered in their work. The values of model parameters are given in Table 1. The experimental results and the model prediction are shown in Figure 2. Both the laboratory data and the DEM simulations are reasonably consistent with the predicted curves.

## 4 | A REFERENCE MODEL FOR FINE GRANULAR MATRIX

It is well recognized that the constitutive relationship of fine matrix is a frame of reference for evaluating the coarse fraction effect of multi-phase composite materials.<sup>16,18</sup> In the sequel, incremental stress-strain relationship will be adopted for describing the deformation behavior of granular matrix. The convention of classical soil mechanics is followed, both the compressive strain and stress are taken as positive.

### 4.1 | General formulations

The elastic stress-strain relationship is given by using hyper-elasticity as

$$d\epsilon_{ijm}^e = C_{ijklm}^e d\sigma'_{klm} \quad (8)$$

with  $C_{ijklm}^e$  being the elastic compliance tensor of matrix:

$$C_{ijklm}^e = \frac{1}{3(1-2\mu_m)K_{em}} [(1+\mu_m)\delta_{ik}\delta_{jl} - \mu_m\delta_{ij}\delta_{kl}] \quad (9)$$

where  $\delta_{ij}$ ,  $\delta_{ik}$ ,  $\delta_{jl}$ , and  $\delta_{kl}$  are Kronecker's symbols,  $\mu_m$  is the Poisson's ratio of the fine granular matrix,  $K_{em}$  is the elastic modulus which is related to the elastic shear stiffness of fine matrix  $G_{em}$ :

$$K_{em} = \frac{1+\mu_m}{3(1-2\mu_m)} G_{em} \quad (10)$$

The elastic shear stiffness of fine granular matrix  $G_{em}$ , which is dependent on the stress level and void ratio, can be approximated by the following function proposed by Hardin and Black<sup>44</sup>:

$$G_{em} = A_m \left( \frac{2.97 - e_m}{1 + e_m} \right)^2 \sqrt{p'_m p_a} \quad (11)$$

where  $A_m$  is a model parameter for the fine granular matrix,  $p_a = 101.3$  kPa is a reference stress,  $e_m$  and  $p'_m$  are the void ratio and the effective mean stress of the fine granular matrix.

The incremental plasticity theory presented by Scott<sup>45</sup> and Pastor et al.<sup>46</sup> has been successfully applied to describe the behavior of various cohesionless soils.<sup>25,47-49</sup> It is adopted herein for the stress-strain relationship of the plastic part of granular matrix:

$$d\epsilon_{ijm}^p = C_{ijklm}^p d\sigma'_{klm} \quad (12)$$

with  $C_{ijklm}^p$  being the plastic compliance tensor of fine granular matrix:

$$C_{ijklm}^p = -\frac{1}{K_{pm}} m_{ijm} n_{klm} \quad (13)$$

where  $K_{pm}$  is the plastic modulus of the fine granular matrix,  $n_{klm}$  and  $m_{ijm}$  are unit vectors, representing the loading direction and flow direction. They are normal to the yield surface and potential surface of fine granular matrix, respectively:

$$m_{ijm} = \frac{\frac{\partial g_m}{\partial \sigma'_{ijm}}}{\sqrt{\frac{\partial g_m}{\partial \sigma'_{ijm}} \frac{\partial g_m}{\partial \sigma'_{ijm}}}}; \quad n_{klm} = \frac{\frac{\partial f_m}{\partial \sigma'_{klm}}}{\sqrt{\frac{\partial f_m}{\partial \sigma'_{stm}} \frac{\partial f_m}{\partial \sigma'_{stm}}}} \quad (14)$$

Substitution of Equations (8), (12) into Equation (1b) gives

$$d\varepsilon_{ijm} = C_{ijklm} d\sigma'_{klm} \quad (15a)$$

$$C_{ijklm} = C_{ijklm}^e + C_{ijklm}^p \quad (15b)$$

## 4.2 | Dilatancy and hardening

The critical-state based models are widely used to reproduce the yield and flow behavior of cohesionless soils.<sup>24,50–53</sup> A versatile yield surface proposed by McDowell and Hau<sup>54</sup> is adopted as the yield surface for the fine granular matrix:

$$f_m : q_m^2 + \frac{M_m^2}{1 - k_m} \left( \frac{p'_m}{p'_{cm}} \right)^{\frac{2}{k_m}} p'_{cm}{}^2 - \frac{M_m^2 p'_{cm}{}^2}{1 - k_m} = 0; (k_m \neq 1) \quad (16)$$

where  $M_m$  and  $k_m$  are critical state parameters,  $q_m$  is the deviatoric stress of the granular matrix,  $p_{cm}$  denotes the size of the yield surface of the granular matrix.

If an associated flow rule is assumed for the fine granular matrix, the plastic potential surface  $g_m$  is the yield surface  $f_m$ . Therefore, the dilatancy function  $d_m$  is

$$d_m = \frac{d\varepsilon_v}{d\varepsilon_s} = \frac{\partial g_m}{\partial p'_m} \left( \frac{\partial g_m}{\partial q_m} \right)^{-1} = \frac{M_m^2 - \eta_m^2}{k_m \eta_m} \quad (17)$$

Note that the aim of this study is to present a compact, reference model for gap-graded granular soils, and its extension to incorporate the non-associative flow which describes the behavior of granular soils better, for example, the fractional order plasticity,<sup>25,49</sup> can be readily made but will be left as a future pursuit. It has been well recognized that the deformation behavior of granular soils is state dependent, for example, the stress level and density of granular soils. A state variable has been proposed by Been and Jefferies<sup>55</sup> to consider the state-dependent effect. It represents the difference between the current void ratio and the void ratio at critical state line at a given stress level.

$$\zeta = e_m - e_{cm} \quad (18)$$

where  $\zeta$  is the state variable, and  $e_{cm}$  is the corresponding void ratio at Critical State Line. The empirical equation proposed by Li and Wang<sup>56</sup> are adopted for the Critical State Line of fine granular matrix:

$$e_{cm} = e_{\Gamma m} - \lambda_m \left( \frac{p'_m}{p_a} \right)^{\chi_m} \quad (19)$$

where  $e_{\Gamma m}$ ,  $\lambda_m$ , and  $\chi_m$  are the critical state parameters, the subscript “m” denotes the fine granular matrix. As noted by Li and Wang,<sup>56</sup> the value of  $\chi_m$  varies in a narrow range (between 0.6 and 0.8).

The dilatancy function  $d_m$  (Equation 17) is revised by incorporating the state variable  $\zeta$ :

$$d_m = \frac{M_m^2 \exp(m\zeta) - \eta_m^2}{k_m \eta_m} \quad (20)$$

where  $m$  is a model parameter,  $\eta_m$  is the ratio of deviatoric stress to effective mean stress of granular matrix. The plastic flow can then be expressed as

$$\frac{\partial g_m}{\partial \sigma'_{ijm}} = \frac{\partial g_m}{\partial q_m} \left( d_m \frac{\partial p'_m}{\partial \sigma'_{ijm}} + \frac{\partial q_m}{\partial \sigma'_{ijm}} \right) \quad (21)$$

The hardening modulus proposed by Li and Dafalias<sup>57</sup> is used in this work:

$$K_{pm} = (h_1 - h_2 e_m) G_{em} \left( \frac{M_p}{\eta_m} - 1 \right) \exp(n\zeta) \quad (22)$$

where  $h_1$ ,  $h_2$ , and  $n$  are model parameters,  $M_p$  is the virtual peak stress ratio:

$$M_p = M_m \exp(-n\zeta) \quad (23)$$

## 5 | CONSTITUTIVE MODEL FOR GAP-GRADED GRANULAR SOILS

For traditional particulate-reinforced materials, the mechanisms governing the elastic and plastic deformation are different. While the internal structure remains the same in elastic range, the change of interfacial transition zone plays an important role as plastic deformation occurs.<sup>58–59</sup> The mechanisms governing the deformation behavior of gap-graded soils is different from that of the traditional composites. Since the fine matrix is cohesionless, the structure change in the vicinity of the interface between fines and aggregate does not play a crucial role in the reinforcement effect. This type of reinforced effect can be well described by Equation (6). It is seen that the overall elastic shear stiffness is approximately close to that of the granular matrix for a negligible coarse fraction. The overall elastic shear stiffness rises with the increasing coarse fraction. When the inter-aggregate structure approaches the minimum packing state, the overall elastic shear stiffness becomes much higher than that of the granular matrix.

The stress-strain relationship of gap-graded granular materials can be expressed as

$$d\varepsilon_{ij} = d\varepsilon_{ij}^e + d\varepsilon_{ij}^p = C_{ijkl} d\sigma'_{kl} \quad (24)$$

with  $C_{ijkl}$  being the overall compliance tensor of gap-graded granular materials:

$$C_{ijkl} = C_{ijkl}^e + C_{ijkl}^p \quad (25)$$

where  $C_{ijkl}^e$  and  $C_{ijkl}^p$  are elastic and plastic compliance tensor of gap-graded soils, respectively. Analogous to the elastic compliance tensor of granular matrix, the overall elastic compliance tensor is given as

$$C_{ijkl}^e = \frac{1}{3(1 - 2\mu_m)K_e} [(1 + \mu_m)\delta_{ik}\delta_{jl} - \mu_m\delta_{ij}\delta_{kl}] \quad (26)$$

with  $K_e$  being the overall elastic shear stiffness of gap-graded granular soils.

Substitution of Equations (10) and (11) into Equation (6) yields

$$K_e = \frac{A_m(1 + \mu_m)}{3(1 - 2\mu_m)} \left( \frac{\bar{\phi}_a}{\bar{\phi}_a - \phi_a} \right)^\xi \left( \frac{2.97 - e_m}{1 + e_m} \right)^2 \sqrt{p'_m p_a} \quad (27)$$

The elastic stiffness of mixtures is modeled using an empirical approach, which may lead to predictions of non-conservative response.<sup>60</sup> As an alternative method, hyperelastic approach can be adopted to describe the elastic response which is consistent with the laws of thermodynamics. However, this may lead to certain complexity in the mathematical treatment.

The overall plastic compliance tensor is expressed as

$$C_{ijkl}^p = -\frac{1}{K_p} m_{ij} n_{kl} \quad (28)$$

where the unit vectors  $n_{kl}$  and  $m_{ij}$  are the overall loading direction and flow direction of gap-graded granular soils:

$$m_{ij} = \frac{\frac{\partial g}{\partial \sigma'_{ij}}}{\sqrt{\frac{\partial g}{\partial \sigma'_{ij}} \frac{\partial g}{\partial \sigma'_{ij}}}}; \quad n_{kl} = \frac{\frac{\partial f}{\partial \sigma'_{kl}}}{\sqrt{\frac{\partial f}{\partial \sigma'_{st}} \frac{\partial f}{\partial \sigma'_{st}}}} \quad (29)$$

where  $f$  and  $g$  are the yield surface and potential surface for the gap-graded granular soils, respectively.

It is well recognized that partial contacts and matrix-bridges between adjacent aggregates are responsible for the reinforced effect of aggregates in gap-graded soils.<sup>11,27,37,38</sup> The loading transmission in inter-aggregate skeleton induces stress concentration within the composite soil, known as the “coarse fraction effect”. As noted by Shi and Yin,<sup>11</sup> for a given gap-graded soil, the reinforcing effect of aggregates uniquely relies on the coarse fraction. Therefore, no matter whether the response is within elastic range or not, the coarse fraction effect as well as loading transmission within inter-aggregate skeleton may remain unchanged. Similar approaches have been adopted by other researchers to predict the overall stiffness of granular mixtures, for example, estimation of stiffness based on elastic strain is generalized to nonlinear elasto-plastic range.<sup>61–63</sup> Analogously, it is assumed that the homogenization law of plastic modulus conforms to the elastic 1, the overall plastic modulus of gap-graded granular soils  $K_p$  is given as

$$K_p = (h_1 - h_2 e_m) G_{em} \left( \frac{M_p}{\eta_m} - 1 \right) \exp(n\zeta) \left( \frac{\bar{\phi}_a}{\bar{\phi}_a - \phi_a} \right)^\xi \quad (30)$$

The plastic strain increment is related to the plastic flow:

$$d\epsilon_{ijm}^p = \vartheta_m \frac{\partial g_m}{\partial \sigma'_{ijm}}; d\epsilon_{ij}^p = \vartheta \frac{\partial g}{\partial \sigma'_{ij}} \quad (31)$$

where  $\vartheta$  and  $\vartheta_m$  are scalars. Substitution of Equations (31) into (2b) reveals that overall plastic flow is in proportion to that of the granular matrix:

$$\frac{\partial g}{\partial \sigma'_{ij}} \propto \frac{\partial g_m}{\partial \sigma'_{ijm}} \quad (32)$$

The flow direction vector is a unit vector, so that

$$m_{ij} = \frac{\frac{\partial g}{\partial \sigma'_{ij}}}{\sqrt{\frac{\partial g}{\partial \sigma'_{ij}} \frac{\partial g}{\partial \sigma'_{ij}}}} = \frac{\frac{\partial g_m}{\partial \sigma'_{ijm}}}{\sqrt{\frac{\partial g_m}{\partial \sigma'_{ijm}} \frac{\partial g_m}{\partial \sigma'_{ijm}}}} = m_{ijm} \quad (33)$$

It is assumed that the rock aggregates are randomly distributed with in the fine granular matrix, an associated flow rule is reasonable to be assumed for the gap-graded granular soils. Therefore, the loading direction is consistent with the flow direction, that is,  $n_{ij} = m_{ij}$ . Note that if there is a preferred orientation of the rock inclusions, the associated flow rule is not suitable, in this case, Equation (33) is questionable.

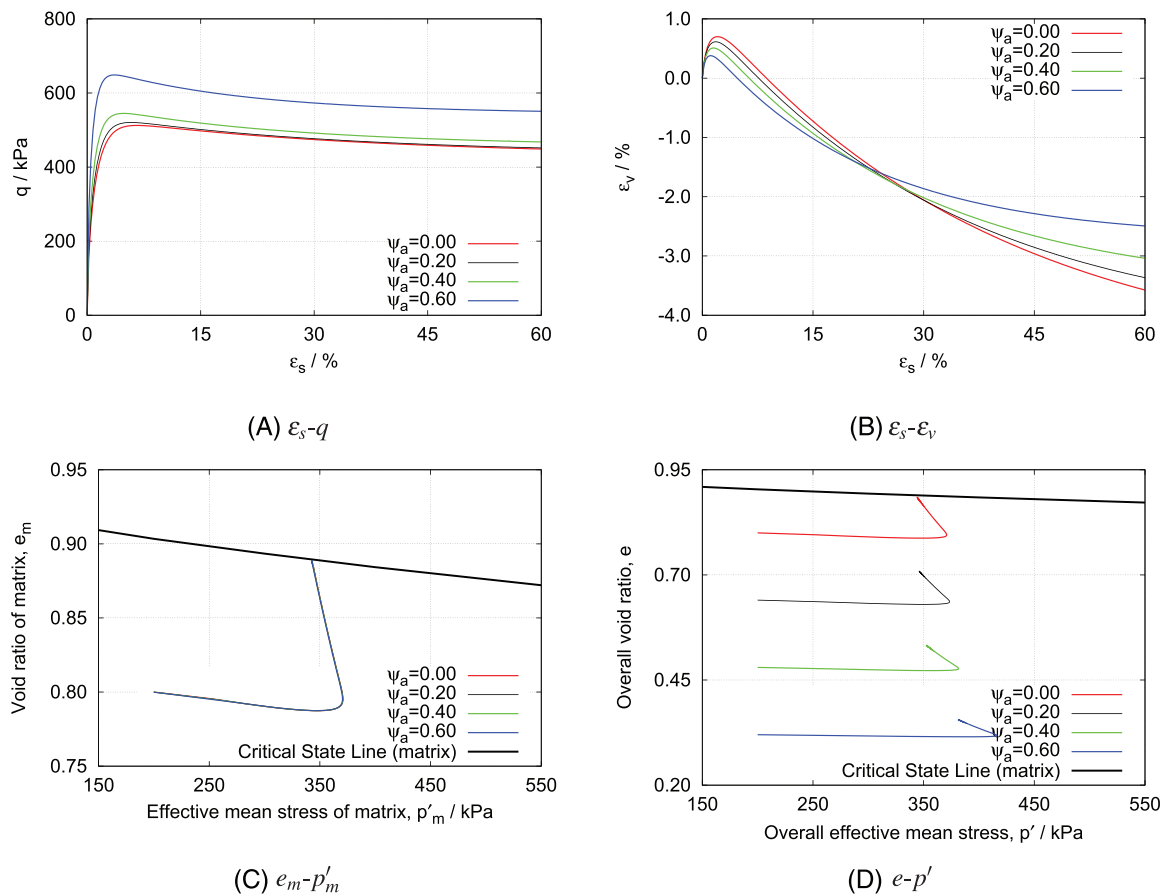
## 6 | MODEL PARAMETERS OF THE PROPOSED MODEL

The proposed model contains 13 parameters:  $A_m, \mu_m, M_m, N_m, \lambda_m, \kappa_m, k_m, m, h_1, h_2, n, \bar{\phi}_a, \xi$ . They can be classified into 5 categories: (1)  $A_m$  and  $\mu_m$  are elastic parameters of the granular matrix; (2)  $M_m, N_m, \lambda_m, \kappa_m$  are critical state parameters,  $M_m$  defines the critical state line in  $p'$ - $q$  stress plane,  $N_m, \lambda_m$ , and  $\kappa_m$  defines the critical state line in  $e$ - $p'$  compression plane. They are calibrated through the critical state data from triaxial tests; (3)  $k_m$  and  $m$  are dilatancy parameters, controlling the state-dependent flow, respectively. (4)  $h_1, h_2$  and  $n$  are hardening parameters. According to Li and Dafalias,<sup>57</sup>  $h_1$  and  $h_2$  can be calibrated from stress-strain curves of drained triaxial tests on granular matrix with different initial densities, and  $n$  can be estimated from the peak stress state of drained triaxial tests; (5)  $\bar{\phi}_a$  and  $\xi$  are structure parameters,  $\bar{\phi}_a$  relies on the minimum density of rock aggregates, and  $\xi$  is suggested to be calibrated using trial and error method.  $A_m, \mu_m, M_m, N_m, \lambda_m, \kappa_m, k_m, m, h_1, h_2$ , and  $n$  are for the constitutive model of the fine granular matrix, which are independent of the internal structure of gap-graded granular mixtures. All of them can be calibrated based on the results of the conventional triaxial tests on the pure fine granular material.  $\xi$  is a structure parameter describing the change of inter-granular skeleton with coarse fraction effect of rock aggregates.



TABLE 2 Model parameters for benchmark analysis and validation of the proposed model

Parameters		Benchmark analysis	Chong-Qing soil	Rock-soil mixture
Elastic parameters	$A_m$	125	120	60
	$\mu_m$	0.20	0.30	0.20
Critical state parameters	$M_m$	1.25	1.31	1.75
	$N_m$	0.934	0.561	0.510
	$\lambda_m$	0.019	0.043	0.024
	$\kappa_m$	0.7	0.6	0.7
Dilatancy parameters	$k_m$	2.0	2.0	5.8
	$M$	0.0	1.1	2.1
Hardening parameters	$h_1$	3.15	1.2	0.59
	$h_2$	3.05	1.8	0.92
	$N$	1.1	15.0	2.1
Structure parameters	$\tilde{\phi}_a$	0.65	0.65	0.65
	$\Xi$	0.70 (0.00,0.35, 1.05)	0.70	0.90/0.72/0.75

FIGURE 3 Simulations of the drained triaxial tests with different coarse fractions using the proposed model: (A) es-q, (B) es- $\varepsilon_v$ , (C)  $e_m$ - $p'_m$ , (D)  $e$ - $p'$ 

## 7 | MODEL ELABORATION

The incremental stress-strain relationship of the proposed model is solved by the linearized integration technique.<sup>64</sup> The incremental stress of the fine granular matrix  $d\sigma'_{jk,m}$  is chose as the principal invariants for elementary simulation. The

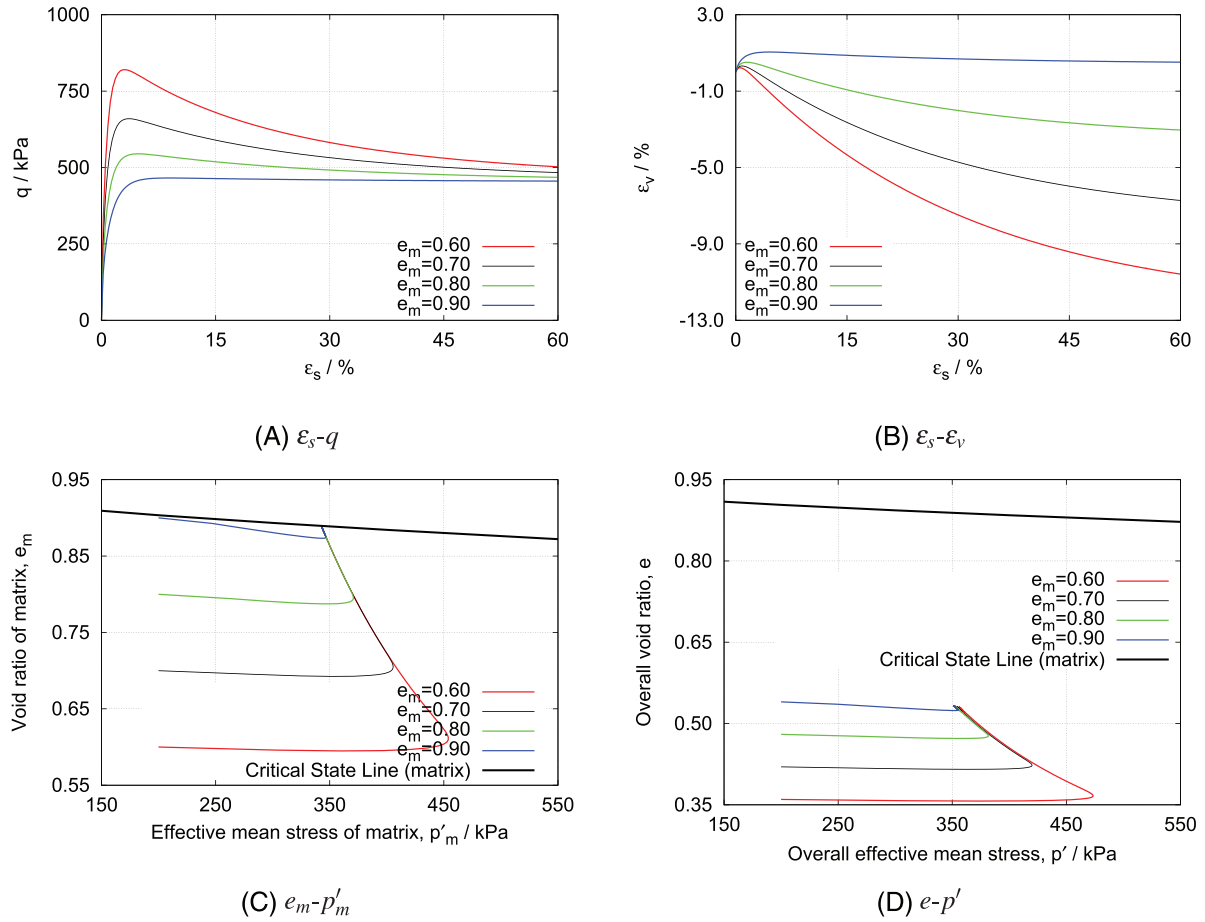


FIGURE 4 Simulations of the drained triaxial tests with different initial density of matrix using the proposed model: (A)  $\varepsilon_s$ - $q$ , (B)  $\varepsilon_s$ - $\varepsilon_v$ , (C)  $e_m$ - $p'_m$ , (D)  $e$ - $p'$

loading constraints for gap-graded granular materials are linearized as:

$$(P_{ist} + Q_{ipq} C_{pqst}) \Theta_{jkst}^{-1} d\sigma'_{jkm} = dY_i \quad (34)$$

where  $P_{ijk}$  and  $Q_{ijk}$  are overall constant coefficients of gap-graded granular materials,  $dY_i$  is a prescribed loading increment at a given incremental step,  $\Theta_{stjk}$  is the stress concentration tensor

$$d\sigma'_{st} = \Theta_{jkst}^{-1} d\sigma'_{jkm} \quad (35)$$

Thanks to the incompressible rock aggregates, the stress concentration tensor can be derived from the overall constitutive relationship (Equation 24) and constitutive relationship of the fine granular matrix (Equation 15b):

$$\Theta_{jkst} = \frac{1}{1 - \phi_a} C_{pqjkm}^{-1} C_{pqst} \quad (36)$$

## 7.1 | Parametric study of the proposed model

Simulation of element tests follows the numerical integration procedure presented by Bardet and Choucair.<sup>64</sup> From the full model of gap-graded granular mixtures, the predicted deformation behavior is associated with the coarse fraction, the initial density of fine granular matrix and value of structure parameter. In the sequel, the effect of coarse fraction (Series-1), initial density of matrix (Series-2), and the influence structure parameter (Series-3) will be evaluated. Simulations of

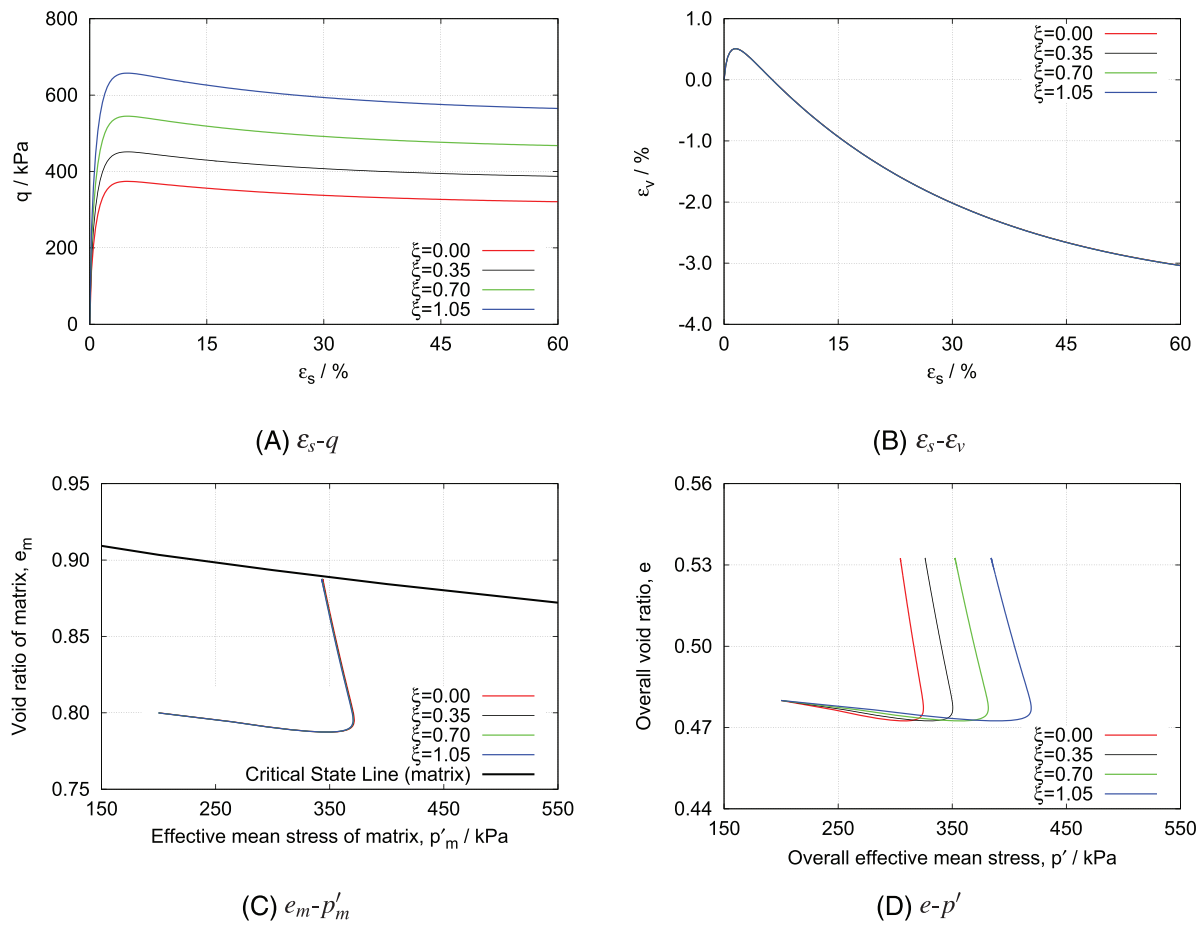


FIGURE 5 Simulations of the drained triaxial tests with different values of the structure parameter using the proposed model: (A)  $\varepsilon_s$ - $q$ , (B)  $\varepsilon_s$ - $\varepsilon_v$ , (C)  $e_m$ - $p'_m$ , (D)  $e$ - $p'$

drained triaxial tests of gap-graded granular materials are done. The assumed values of model parameters are listed in Table 2.  $k_m = 2$  is assigned for the potential surface of the granular matrix, and  $m = 0$  is adopted for the state-dependent flow. So that, the potential surface and flow direction are reduced to those in the Modified Cam clay model. The minimum void ratio of rock aggregates is assumed to be 0.54, and the rock aggregates and fine particles have the same particle density. The Poisson's ratio is assumed to be 0.20. The other model parameters are the same as the values for Toyoura sand.<sup>57</sup>

The simulation of drained triaxial tests of gap-graded granular materials with various rock fractions (Series-1) are shown in Figure 3. The initial void ratio is assumed to be 0.80, and  $\xi = 0.70$  is assigned for the structure parameter. Four rock fractions are considered (0.0, 0.2, 0.4, 0.6). It is seen that the initial shear stiffness increases as the rock fraction rises, which is consistent with Equation (27). Both the peak shear strength and the residual shear strength increases with the increasing rock fraction, indicating a positive reinforcement of coarse inclusions. The volumetric deformation of gap-graded granular materials reveals that the coarse fraction has a negative influence on the overall deformation, including both the compressive and dilative ones. The change of void ratio of granular matrix and overall void ratio are shown in Figure 3C and Figure 3D, respectively. There is a unique relationship between the void ratio of granular matrix  $e_m$  and  $p'_m$  compression plane. The void ratio  $e_m$  shows a slight decrease, and a further increase towards the critical state line of the fine granular matrix. The initial overall void ratio of gap-graded soils lies below that of the pure granular matrix, and the overall void ratio at the critical state decreases with rising rock fraction. This indicates that the coarse fraction has a significant influence on the critical state of gap-graded granular materials.

The effect of initial density on the behavior of gap-graded granular soils is also evaluated, and the simulated results are shown in Figure 4. The rock fraction is assumed to be 0.40, and  $\xi = 0.70$  is assigned in all the simulations, and 4 different initial void ratios of the granular matrix, 0.60, 0.70, 0.80, and 0.90, are considered (Series-2). It is seen that both the overall initial stiffness and the peak shear strength increases with decreasing initial void ratio of matrix. The shear dilatancy reduces as the void ratio of matrix increases. The deformation behavior in compression plane (Figure 4C and Figure 4D)

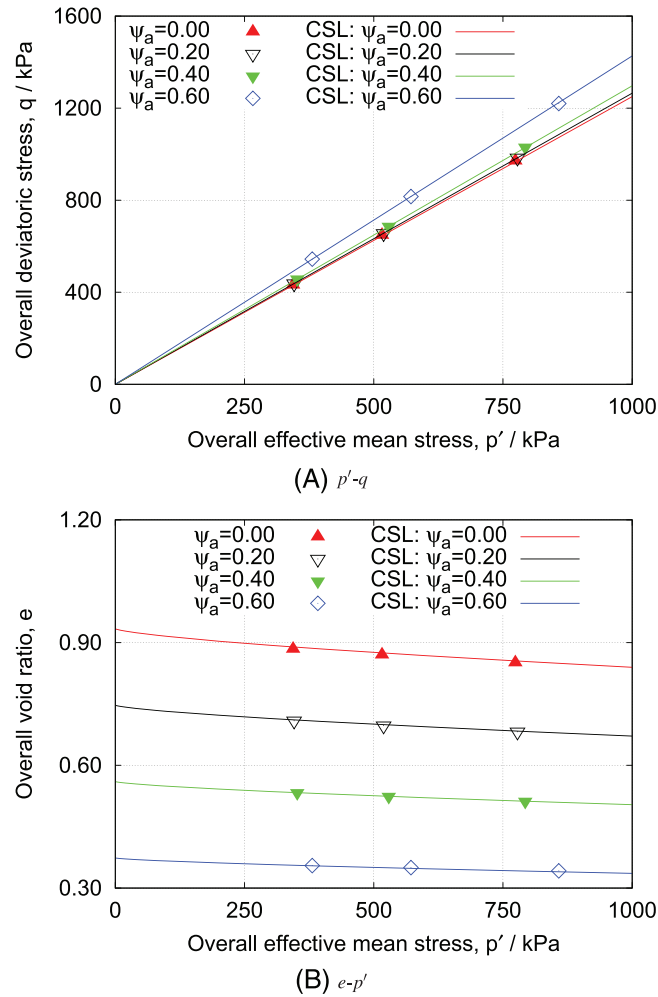


FIGURE 6 Critical state of granular mixtures with different coarse fractions: (A)  $p_0$ - $q$ , (B)  $e$ - $p_0$

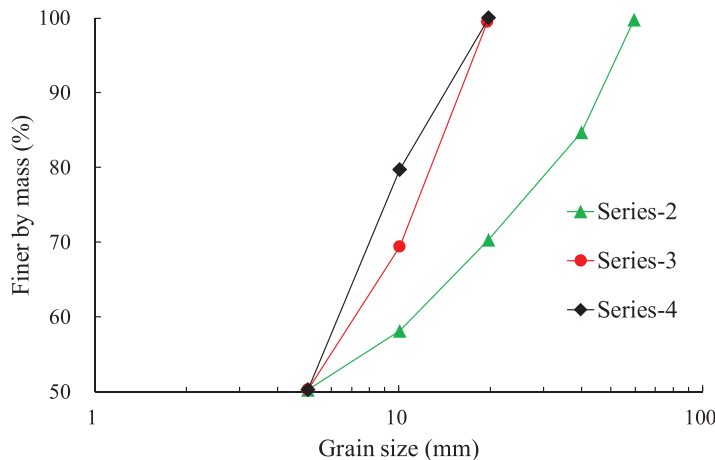
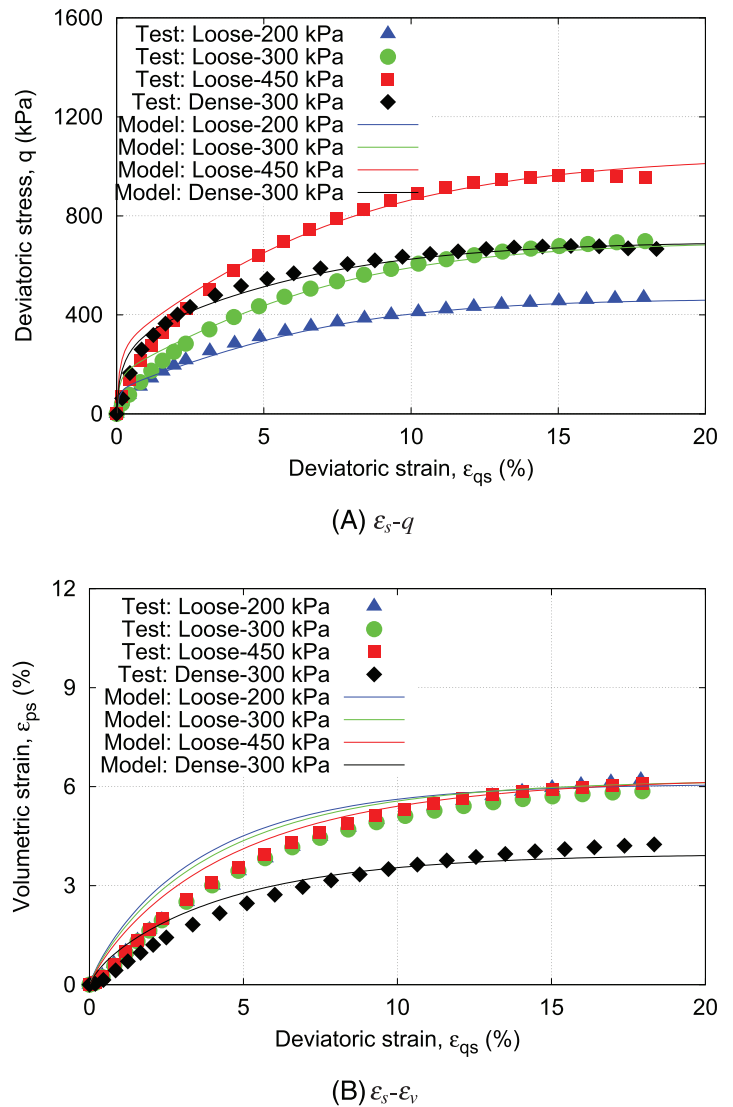


FIGURE 7 Grain size distribution of rock aggregates of rock-soil mixtures (data cited from Zhang et al., 2016)

reveals that the void ratio of granular matrix converges to the critical state line of pure matrix. However, the critical state points of gap-graded granular soils are located below the critical state line of matrix due to the coarse inclusions.

To investigate the effect of structure parameter, the initial void ratio and the rock fraction are assumed to be 0.80 and 0.40, respectively. Four different values of structure parameter, 0.00, 0.35, 0.70, 1.05, are considered (Series-3), and the results are summarized in Figure 5. The structure parameter significantly affects the overall response of gap-graded granular soils. The initial stiffness, the peak shear strength and the critical state shear strength increase with the increas-

**FIGURE 8** Experimental stress-strain data and numerical simulations of pure sand matrix (Chong- Qing soil): (A) es-q, (B) es-ev

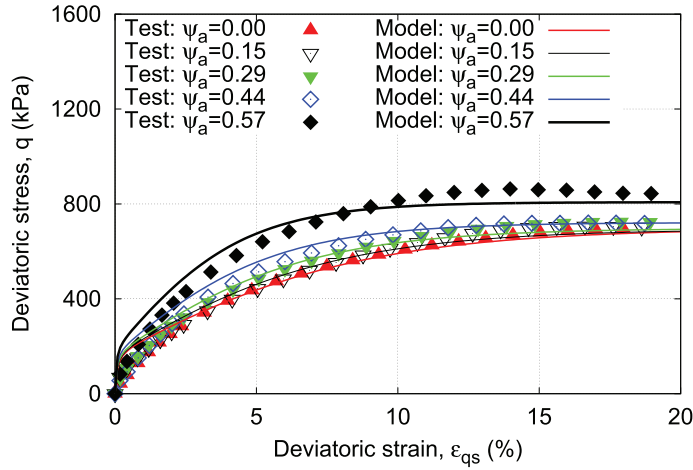
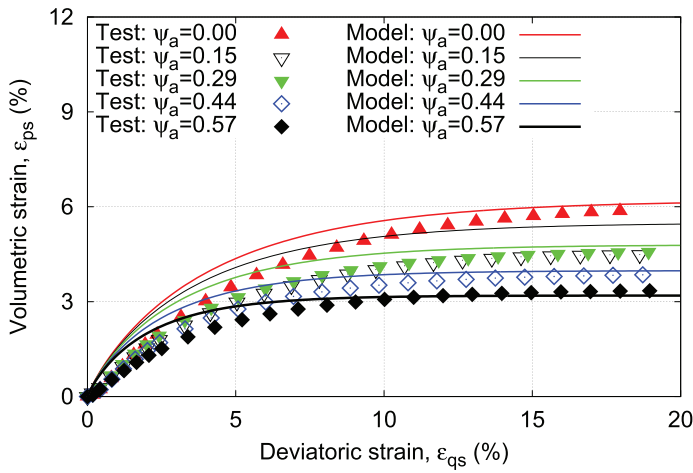


ing structure parameters, that is, a higher value of structure parameter indicates a more distinct coarse fraction effect of rock aggregates. The overall volumetric strain is almost unique, indicating a negligible influence of structure parameter on the volume change of gap-graded granular materials. As a result, the critical state void ratio of granular matrix is the same regardless of the value of structure parameter (Figure 5D). Analogous to the coarse fraction effect, the change of void ratio of granular matrix is unique in  $e_m$  and  $p'_m$  compression plane (Figure 5C).

## 7.2 | Critical state lines

The influence coarse fraction on the critical state line of gap-graded is crucial for engineers. The model parameters for the simulations are the same as Series-2. The results of critical state points for gap-graded soils with different rock fractions and at different confining pressures are summarized and shown in Figure 6. It is seen that the critical state points of gap-graded granular soils can be well fitted by a straight line through the origin for a given rock fraction, and the critical state parameter  $M_m$  increases with the rock fraction (Table 2).  $M_m$  increases from 1.25 to 1.43 as the rock fraction rises to 0.60. The critical state points in  $e$  and  $p'$  compression plane show a decreasing void ratio with increasing coarse fraction. Both  $N_m$  and  $\lambda_m$  fall as the coarse fraction increases (Table 3). It is assumed that the effective mean stress in the matrix is the same as the overall effective mean stress, Equation (19) is revised as

$$e_{cm} = e_{\Gamma m} - \lambda_m \left( \frac{p'}{p_a} \right)^{\chi_m} \quad (37)$$

(A)  $\varepsilon_s$ - $q$ (B)  $\varepsilon_s$ - $\varepsilon_v$ 

**FIGURE 9** Experimental stress-strain data and numerical simulations of granular mixtures with loose matrix: (A)  $\varepsilon_s$ - $q$ , (B)  $\varepsilon_s$ - $\varepsilon_v$

As noted by Shi et al.,<sup>18</sup> the void ratio of the fine granular matrix can be formulated as a function of the overall void ratio and the rock fraction:

$$e_{cm} = \frac{e_c \rho_m}{(1 - \psi_a) \rho} \quad (38)$$

If it is assumed that the particle density of the matrix and aggregates are the same, Equation (38) can be simplified as

$$e_{cm} = \frac{e_c}{1 - \psi_a} \quad (39)$$

Substitution of Equation (39) into (37), it follows:

$$e_c = e_\Gamma - \lambda \left( \frac{p'}{p_a} \right)^{\chi_m} \quad (40)$$

with  $e_\Gamma$  and  $\lambda$  being the equivalent critical state parameters of the gap-graded granular soils:

$$e_\Gamma = (1 - \psi_a) e_{\Gamma m} \quad (41a)$$

$$\lambda = (1 - \psi_a) \lambda_m \quad (41b)$$

**FIGURE 10** Experimental stress-strain data and numerical simulations of granular mixtures with dense matrix: (A) es-q, (B) es- $\epsilon_v$

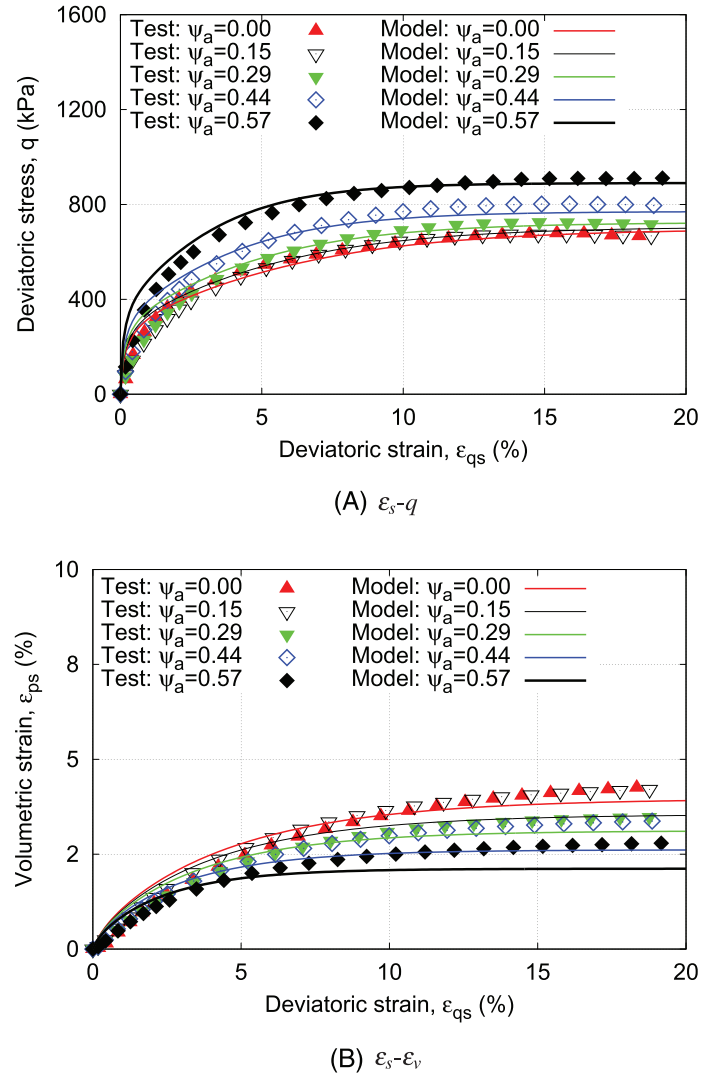


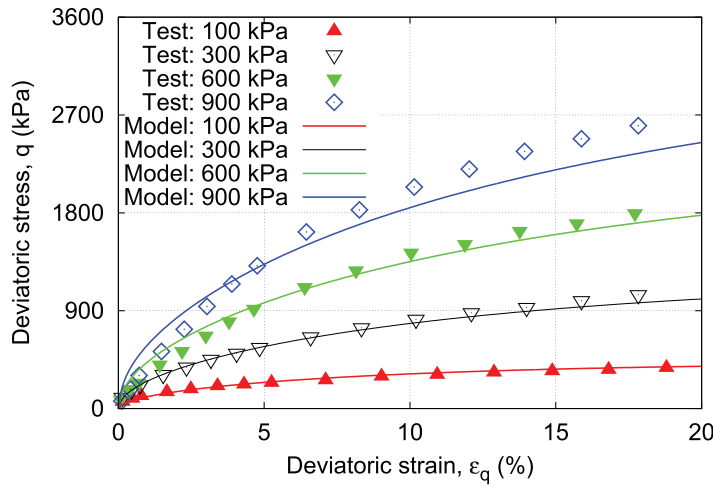
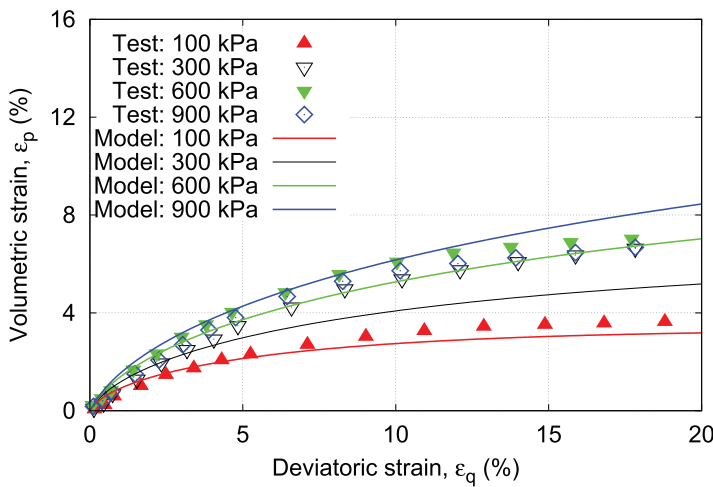
**TABLE 3** Simulation and estimation of critical state parameters of granular mixtures

Coarse fraction	0.00	0.20	0.40	0.60
$N_m$ (Simulation)	0.934	0.744	0.559	0.374
$\lambda_m$ (Simulation)	0.019	0.015	0.011	0.007
$M_m$ (Simulation)	1.25	1.27	1.36	1.43
$N_m$ (Estimation)	0.934	0.747	0.560	0.374
$\lambda_m$ (Estimation)	0.019	0.015	0.011	0.008

The values of parameters calibrated from simulations and estimated from Equation (41) are listed in Table 3 denoted as “simulation” and “estimation,” respectively. The parameters based on simulated results is well consistent with Equation (41). Hence, Equations (40) and (41) gives a practical estimation of the critical state line of gap-graded granular soils with a coarse fraction below 0.60. Note that in case of a relatively high coarse fraction, the stress in fine granular matrix may be significantly lower than the overall value, and therefore this estimation is not reliable any more.

## 8 | VALIDATION OF THE PROPOSED MODEL

As discussed in the previous section, the behavior of gap-graded granular soils is affected by the coarse fraction and density of fine granular matrix. The particle shape and particle size distribution of the coarse aggregates also affect the overall

(A)  $\varepsilon_s$ - $q$ (B)  $\varepsilon_s$ - $\varepsilon_v$ 

**FIGURE 11** Experimental stress-strain data and numerical simulations of pure soil matrix (Series-1): (A)  $\varepsilon_s$ - $q$ , (B)  $\varepsilon_s$ - $\varepsilon_v$

deformation behavior.<sup>2,65,66</sup> The simulated results of Series-3 indicate that the influence of the above factors on the coarse fraction effect can be reproduced by assigning various values of the structure parameter. For validation of the proposed model, the results of 2 gap-graded granular materials from literature are used: (1) the triaxial compression data of sand-gravel mixtures reported by Shi et al.<sup>67</sup>; (2) the triaxial test results of soil-rock mixtures obtained by Zhang et al.<sup>66</sup>

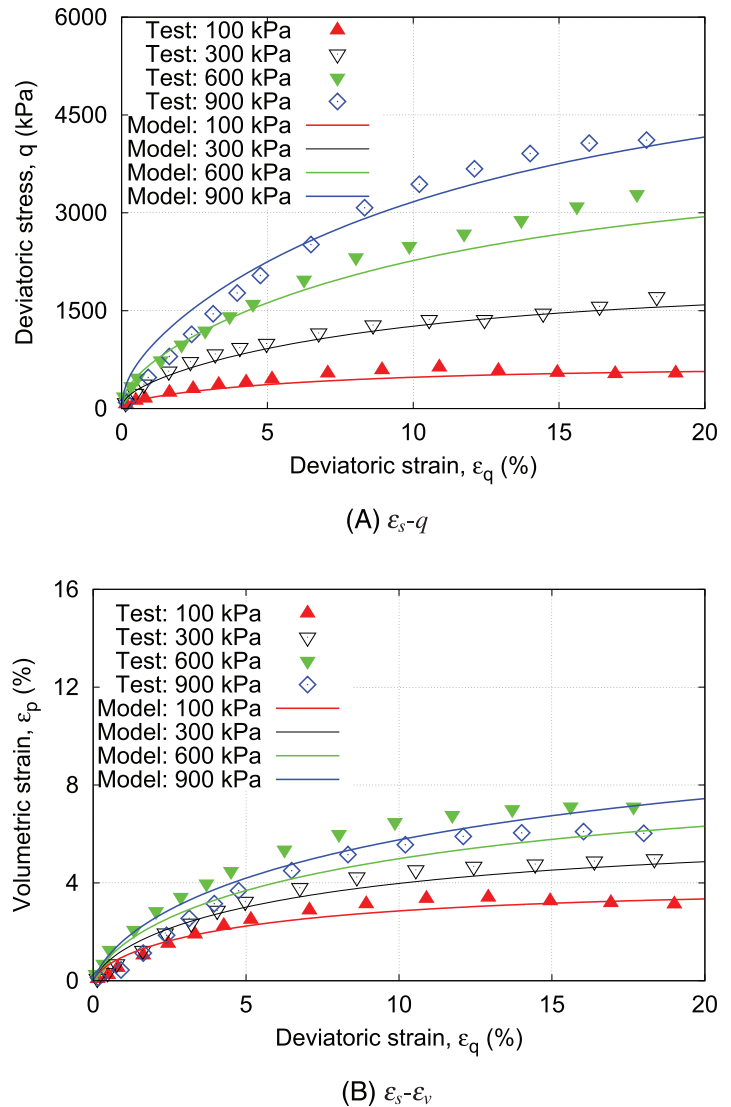
## 8.1 | Sand-gravel mixtures

Chongqing soil is a typical gap-graded soil, which has a deficiency of particle size ranging from 0.425 to 2.0 mm (see Figure 1). The sand particle is the matrix and the coarse gravel is the inclusion. Since the gravels are weak due to weathering factors, it may collapse during the testing process. Therefore, feldspar gravels are used to replace the weathered aggregates. The density of fines is 2.73 mg/m<sup>3</sup>. The minimum and maximum void ratio of fine granular matrix are 0.406 and 1.323, respectively. It has an optimum moisture content of 12% and a maximum dry density of 1.94 mg/m<sup>3</sup>. The diameter of the fines is mostly higher than 0.002 mm, denoting a negligible clay fraction. The coarse gravel has a density of 2.65 mg/m<sup>3</sup>. It has a subangular to angular shape and the diameter varies between 2.0 and 20 mm.

Two series of triaxial tests are adopted for validation of the proposed model. The first Series is a mixture of loose sand and coarse gravels, and the second is a mixture of dense sand and gravels. The initial void ratios of granular matrix are 0.695 and 0.570, respectively. Five various coarse fractions are considered in both 2 series: the first Series (loose matrix, 0.000, 0.153, 0.291, 0.439, 0.569) and the second Series (dense matrix, 0.000, 0.141, 0.276, 0.420, 0.550).



**FIGURE 12** Experimental stress-strain data and numerical simulations of rock-soilmixtures (Series-2): (A) es-q, (B) es-ev



## 8.2 | Soil-rock mixtures

The soil-rock mixtures were taken from a Barrier dam in Sichuan Province, China. As defined by the authors,<sup>66</sup> a diameter of 5 mm was adopted as a threshold to distinguish the “soil” and “rock”: soil particles less than 5 mm in size is denoted “soil” matrix, and coarse aggregate greater than 5 mm in size is represented as “rock” inclusion. The natural water content of the mixture is 10.4%, and the corresponding density is 1.73 mg/m<sup>3</sup>. The natural state is used as the initial state of the mixture samples. Since the soil matrix are induced from the disintegration of the rock blocks, it is reasonable to assume that the 2 phases have the same particle density. Note that, the mixture cannot reach a rather dense state in the laboratory, since ideal mixing is rarely achieved in artificial systems. Hence, gap-graded samples may commonly show strain-hardening behavior.<sup>2,37,66</sup>

Four series of triaxial tests were done by the authors: (1) Series-1, drained triaxial tests on pure soil matrix, which provides a reference for assessing the behavior of soil-rock mixtures; (2) Series-2, drained triaxial tests on rock-soil mixtures, with the size of rock inclusions varying between 5 and 60 mm; (3) Series-3, drained triaxial tests on rock-soil mixtures, with the size of rock inclusions varying between 5 and 20 mm; (4) Series-4, drained triaxial tests on rock-soils mixtures, with the size of rock inclusions varying between 5 and 20 mm. The grain size distribution of rock aggregates is shown in Figure 7. It is seen that the rock content of aggregate in vicinity of 10 mm in Series-3 is lower than that in Series-4. All the samples in triaxial tests has a rock inclusion of 0.50, and they are tested under 4 effective confining stresses, 100, 300, 600, and 900 kPa.

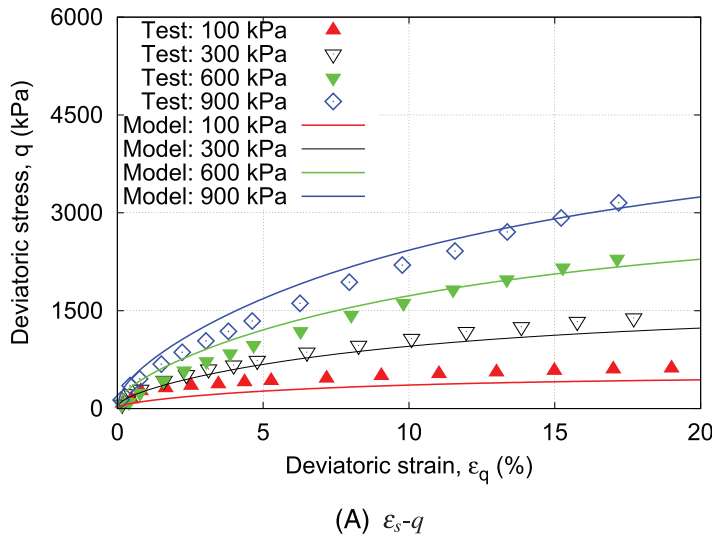
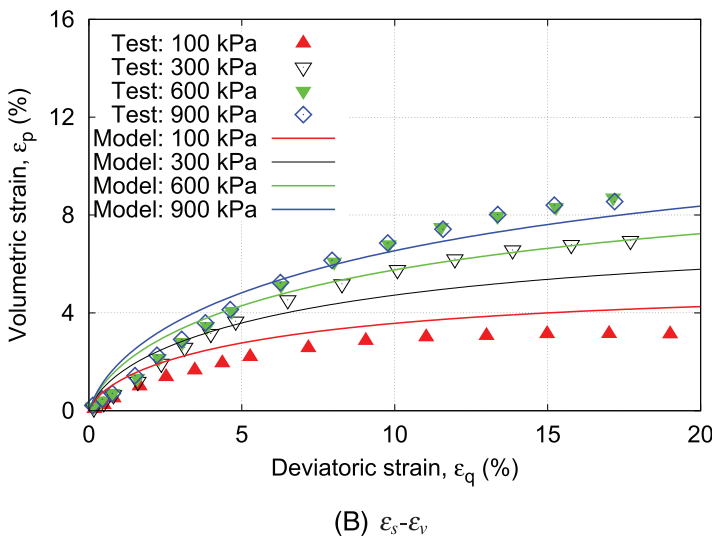


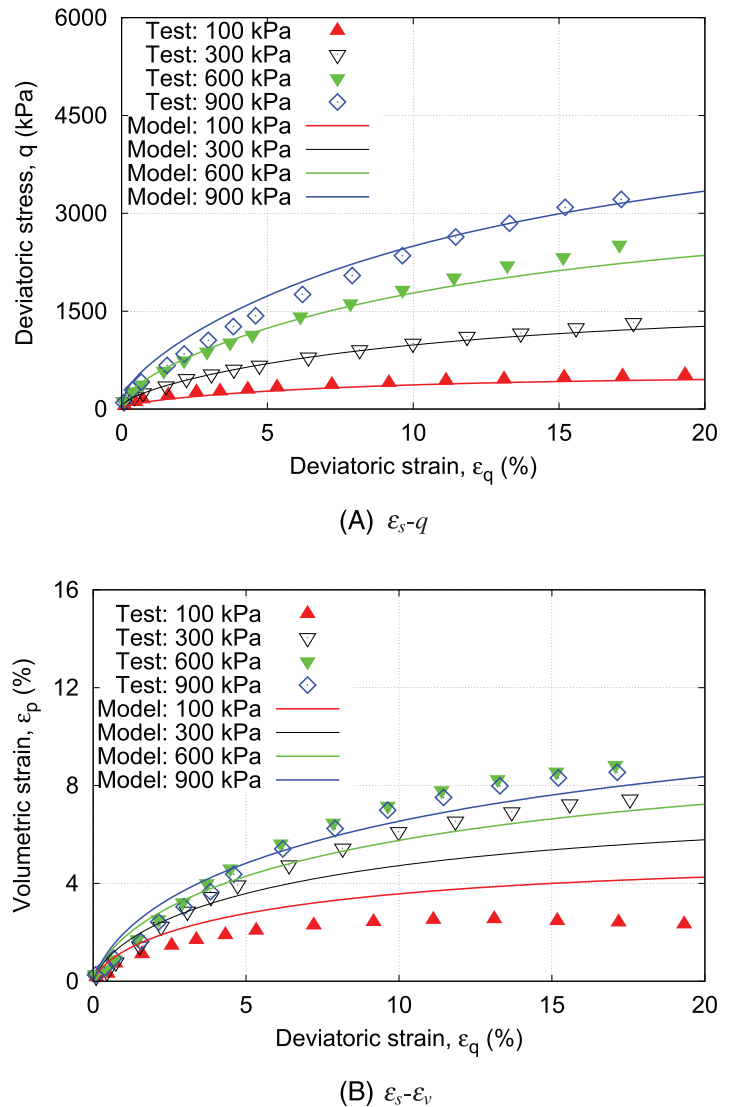
FIGURE 13 Experimental stress-strain data and numerical simulations of rock-soil mixtures (Series-3): (A) es-q, (B) es-ev



### 8.3 | Model predictions on gap-graded granular mixtures

The values of model parameters for the sand-gravel mixtures and soil-rock mixtures are given in Table 1. They are calibrated from the procedures summarized in Section 6. The minimum void ratio of the rock aggregates in above gap-graded materials is not given in the literature. It is assumed to be 0.54, which is a typical value for granular materials with a subangular shape.<sup>68</sup> Therefore, the value of structure parameter  $\tilde{\phi}_a$  is assigned as 0.65. The value of the dilatancy parameter  $k_m$  is as high as 5.8, indicating a distinct difference from the potential surface of the Modified Cam-clay model. The value of the structure parameter  $\xi$  for the sand-gravel mixtures is 0.70, and those for the soil-rock mixtures are 0.90, 0.72, 0.75 for Series-2, Series-3, and Series-4, respectively. The mechanism governing the internal structure of gap-graded granular materials is incorporated into the model by introducing the structure parameter  $\xi$ . The particle shape, particle size and particle size distribution of rock aggregates may affect (1) the partial contacts between rock aggregates, and (2) the sand bridges due to the densified sand matrix between adjacent rock aggregates.<sup>11,18,37</sup> Therefore, different values of structure parameter are adopted for the mixtures. The tests of rock-soil mixtures after Zhang et al.<sup>66</sup> were performed under unsaturated condition with a natural water content of 10.4%. As noted by Zhang,<sup>69</sup> the initial water content is relatively low, so that the water drained out of the sample is negligible, that is, the water content is kept constant during consolidation and shearing process. Both the air pressure and excess pore water pressure are negligible. In this case, the deformation behavior under drained condition can be modelled by assuming constant degree of saturation.

**FIGURE 14** Experimental stress-strain data and numerical simulations of rock-soilmixtures (Series-4): (A) es-q, (B) es-ev



Comparisons between the proposed model and the experimental data of pure sand matrix and sand-gravel mixtures from literature<sup>67</sup> are shown in Figures 8–10. It is seen that the model predictions are consistent with mechanical responses of both pure sand and mixtures, including both the change of mobilized shear strength and volumetric deformation. This reveals that the model can well reproduce the effect of initial density of sand matrix and coarse fraction of sand-gravel mixtures. The numerical predictions of the pure soil matrix soil-rock mixtures using our model are shown in Figures 11–14. It is seen that the model can quantitatively describe the stress-strain curves measured in laboratory (test data from Zhang et al.<sup>66</sup>), regardless of the particle size and particle size distribution of the rock aggregates. The volumetric deformation of the soil-rock mixtures is slightly underestimated in some of the tests. This may have been caused by use of associated flow rule in our model. Extensions of the model incorporating the non-associative flow can be done by introducing additional parameters. However, the associated plastic assumption greatly enhances the tractability and greatly reduces the complexity of the model.

In this work, we focus on granular mixtures with fine-dominated structure. The threshold distinguishing the relative dominance of fines and aggregates is noted as the transitional coarse content (defined in Equation 7), which is characterized by the maximum packing state of coarse aggregate. According to site investigation,<sup>70–72</sup> coarse fraction of mixed soils in reclamation, dredging activities, and weathered areas is usually below the transitional coarse content. Therefore, the soils can be characterized as fine-dominated structure, and their behavior can be well reproduced using the proposed model.

## 9 | CONCLUSIONS

A homogenization-based model has been proposed for gap-graded granular materials within elastoplastic framework. Simulations and validation have been done to present the features and capability of the proposed model which are summarized as follows:

1. A structure parameter related to the internal structure of gap-graded granular materials is incorporated into the proposed model. It varies with the particle shape, particle size, and particle size distribution of rock aggregates. The partial contacts between rock aggregates and the sand bridges composed of densified matrix are responsible for the mechanism governing the internal structure change of gap-graded granular materials.
2. The initial stiffness and peak shear strength rely on both the coarse fraction and the initial density of granular matrix. However, the critical state is irrelevant to the initial state of matrix. The coarse fraction has a negative influence on the overall deformation, including both the compressive and dilative ones.
3. The initial stiffness, peak shear strength and residual shear strength increases with rising structure parameter, that is, a higher value of structure parameter indicates a more significant coarse fraction effect of rock aggregates. However, it has a negligible influence on the volume change of gap-graded granular materials.
4. For gap-graded granular material with a given coarse fraction, the critical state points can be well fitted by a straight line through the origin, and the critical state parameter  $M_m$  increases with the rock fraction. The other two critical state parameters,  $N_m$  and  $\lambda_m$ , fall as the coarse fraction increases. Based on reasonable assumptions, a practical method is proposed for the critical state line in  $e-p'$  compression plane
5. A modified potential surface and a new state-dependent dilatancy function are introduced to describe the dilatancy behavior of granular matrix. Then, a novel homogenization equation is incorporated into the proposed model. It can well reproduce the stress-strain relationship and volumetric deformation behavior of sand-gravel mixtures and soil-rock mixtures.

## ACKNOWLEDGMENTS

This study was partially supported by the National Natural Science Foundation of China (under Grant no. 51679207; 51908193), the Fundamental Research Funds for the Central Universities (under Grant no. B200201050), and the Research Grants Council of Hong Kong (under RGC/GRF Grant no. 16201419, TBRG Grant no. T22-603/15N and CRF Grant no. C6012-15G). The first author appreciates the funding support from VPRG Office of HKUST for his Research Assistant Professor (RAP) position.

## DATA AVAILABILITY STATEMENT

Some or all data, models, or code that support the findings of this study are available from the corresponding author upon reasonable request.

## ORCID

X. S. Shi  <https://orcid.org/0000-0002-6148-1720>

Jidong Zhao  <https://orcid.org/0000-0002-6344-638X>

Yufeng Gao  <https://orcid.org/0000-0002-5837-3382>

## REFERENCES

1. Chen WB, Borana L, Feng WQ, Yin JH, Liu K. Influence of matric suction on nonlinear time-dependent compression behaviour of a granular fill material. *Acta Geotech.* 2019;13:1-19.
2. Ruggeri P, Segato D, Fruzzetti VME, Scarpelli G. Evaluating the shear strength of a natural heterogeneous soil using reconstituted mixtures. *Géotechnique.* 2016;66(11):941-946.
3. Liu D, Cui Y, Guo J, Yu Z, Chan D, Lei M. Investigating the effects of clay/sand content on depositional mechanisms of submarine debris flows through physical and numerical modeling. *Landslides.* 2020;17(8):1863-1880.
4. Qin CB, Chian SC. Kinematic analysis of seismic slope stability with a discretisation technique and pseudo-dynamic approach: a new perspective. *Géotechnique.* 2017;68(6):492-503.
5. Peng D, Xu Q, Liu F, et al. Distribution and failure modes of the landslides in Heitai terrace, China. *Eng. Geol.* 2018;236:97-110.
6. Chandler RJ. The Third Glossop Lecture: clay sediments in depositional basins: the geotechnical cycle. *Q. J. Eng. Geol. Hydrogeol.* 2000;33(1):7-39.

7. Chen WB, Liu K, Yin ZY, Yin JH. Crushing and flooding effects on one-dimensional time-dependent behaviors of a granular soil. *Int. J. Geomech.* 2019;13:04019156.
8. Cui YF, Jiang Y, Guo CX. Investigation of the initiation of shallow failure in widely graded loose soil slopes considering interstitial flow and surface runoff. *Landslides.* 2019;16(4):815-828.
9. Cui YF, Yan Y, Jian G, Sheng H, Wang Z, Yin S. Landslide reconstruction using seismic signal characteristics and numerical simulations: case study of the 2017 "6.24" Xinmo landslide. *Eng. Geol.* 2020:105582.
10. Peters JF, Berney IV ES. Percolation threshold of sand-clay binary mixtures. *J. Geotech. Geoenviron. Eng.* 2010;136(2):310-318.
11. Shi XS, Yin J. Experimental and theoretical investigation on the compression behavior of sand-marine clay mixtures within homogenization framework. *Computers Geotech.* 2017;90:14-26.
12. Tan DY, Yin JH, Feng WQ, Zhu ZH, Qin JQ, Chen WB. New simple method for calculating impact force on flexible barrier considering partial muddy debris flow passing through. *J. Geotech. Geoenviron. Eng.* 2019;145(9):04019051.
13. Zhou Z, Yang H, Wang X, Liu B. Model development and experimental verification for permeability coefficient of soil-rock mixture. *Int. J. Geomech.* 2017;17(4):04016106.
14. Monkul MM, Ozden G. Compressional behavior of clayey sand and transition fines content. *Eng Geol.* 2007;89(3):195-205.
15. Vallejo LE, Mawby R. Porosity influence on the shear strength of granular material-clay mixtures. *Eng. Geol.* 2000;58(2):125-136.
16. Shi XS, Zhao J, Yin J, Yu Z. An elastoplastic model for gap-graded soils based on homogenization theory. *Int. J. Solids Struct.* 2019;163:1-14.
17. Shi XS, Herle I, Muir Wood D. A consolidation model for lumpy composite soils in open-pit mining. *Géotechnique.* 2018;68(3):189-204.
18. Shi XS, Nie J, Zhao J, Gao Y. A homogenization equation for the small strain stiffness of gap-graded granular materials. *Computers Geotech.* 2020;121:103440.
19. Vallejo LE. Interpretation of the limits in shear strength in binary granular mixtures. *Can. Geotech. J.* 2001;38(5):1097-1104.
20. Ueda T, Matsushima T, Yamada Y. Effect of particle size ratio and volume fraction on shear strength of binary granular mixture. *Granul. Matter.* 2011;13(6):731-742.
21. Zhang ZF, Ward AL, Keller JM. Determining the porosity and saturated hydraulic conductivity of binary mixtures. *Vadose Zone J.* 2011;10(1):313-321.
22. Ng TT, Zhou W, Chang XL. Effect of particle shape and fine content on the behavior of binary mixture. *J. Eng. Mech.* 2016;143(1):C4016008.
23. Choo H, Lee W, Lee C, Burns SE. Estimating porosity and particle size for hydraulic conductivity of binary mixed soils containing two different-sized silica particles. *J. Geotech. Geoenviron. Eng.* 2017;144(1):04017104.
24. Gao ZW, Zhao JD. Constitutive modeling of artificially cemented sand by considering fabric anisotropy. *Computers Geotech.* 2012;41:57-69.
25. Sun Y, Gao Y, Zhu Q. Fractional order plasticity modelling of state-dependent behaviour of granular soils without using plastic potential. *Int. J. Plast.* 2018;102:53-69.
26. Zhao S, Evans TM, Zhou X. Effects of curvature-related DEM contact model on the macro-and micro-mechanical behaviours of granular soils. *Géotechnique.* 2018;68(12):1085-1098.
27. Deng Y, Wu Z, Cui Y, Liu S, Wang Q. Sand fraction effect on hydro-mechanical behavior of sand-clay mixture. *Appl. Clay Sci.* 2017;135:355-361.
28. Elkady TY, Shaker AA, Dhowain AW. Shear strengths and volume changes of sand-attapulgitic clay mixtures. *Bull. Eng. Geol. Environ.* 2015;74(2):595-609.
29. Shi XS, Gao YF, Ding JW. Estimation of the compression behavior of sandy clay considering sand fraction effect based on equivalent void ratio concept. *Eng. Geol.* 2021;280:105930.
30. Ji B, Wang T. Plastic constitutive behavior of short-fiber/particle reinforced composites. *Int. J. Plast.* 2003;19(5):565-581.
31. Ng TT. Behavior of ellipsoids of two sizes. *J. Geotech. Geoenviron. Eng.* 2004;130(10):1077-1083.
32. Ng TT, Zhou W, Ma G, Chang XL. Macroscopic and microscopic behaviors of binary mixtures of different particle shapes and particle sizes. *Int. J. Solids Struct.* 2018;135:74-84.
33. Weng GJ. The overall elastoplastic stress-strain relations of dual-phase metals. *J. Mech. Phys. Solids.* 1990;38(3):419-441.
34. González C, Segurado J, LLorca J. Numerical simulation of elasto-plastic deformation of composites: evolution of stress microfields and implications for homogenization models. *J. Mech. Phys. Solids.* 2004;52(7):1573-1593.
35. Liu J, Nicot F, Zhou W. Sustainability of internal structures during shear band forming in 2D granular materials. *Powder Tech.* 2018;338:458-470.
36. De Boer R, Ehlers W. On the problem of fluid and gas-filled elasto-plastic solids. *Int. J. Solids Struct.* 1986;22(11):1231-1242.
37. Jafari MK, Shafiee A. Mechanical behavior of compacted composite clays. *Can. Geotech. J.* 2004;41(6):1152-1167.
38. Chu C, Wu Z, Deng Y, Chen Y, Wang Q. Intrinsic compression behavior of remolded sand-clay mixture. *Can. Geotech. J.* 2017;54(7):926-932.
39. Hill R. A self-consistent mechanics of composite materials. *J. Mech. Phys. Solids.* 1965;13(4):213-222.
40. Mori T, Tanaka K. Average stress in matrix and average elastic energy of materials with misfitting inclusions. *Acta Metallurgica.* 1973;21(5):571-574.
41. Lielens G, Pirotte P, Courniot A, Dupret F, Keunings R. Prediction of thermo-mechanical properties for compression moulded composites. *Compos. Part A: App. Sci. Manuf.* 1998;29(1-2):63-70.
42. González-Hurtado J, Newson T. Measuring the small-strain elastic modulus of gap-graded soils using an effective-medium model and the resonant column apparatus. *Geo-Quebec 2015. Challenges from North to South:* 2015.

43. Ruan B, Miao Y, Cheng K, Yao EL. Study on the small strain shear modulus of saturated sand-fines mixtures by bender element test. *Euro. J. Environ. Civil Eng.* 2018;1-11.
44. Hardin BO, Black WL. Sand stiffness under various triaxial stresses. *J. Soil Mech. Found Div.* 1966;92:27-42.
45. Scott RF. Plasticity and constitutive relations in soil mechanics (the nineteenth terzaghi lecture). *J. Geotech Eng.* 1985;111(5):559-605.
46. Pastor M, Zienkiewicz OC, Chan AHC. Generalized plasticity and the modelling of soil behaviour. *Int. J. Numer. Anal. Methods Geomech.* 1990;14(3):151-190.
47. Bolzon G, Schrefler BA, Zienkiewicz OC. Elastoplastic soil constitutive laws generalized to partially saturated states. *Géotechnique.* 1996;46(2):279-289.
48. Kavvasdas M, Amorosi A. A constitutive model for structured soils. *Géotechnique.* 2000;50(3):263-273.
49. Sun Y, Shen Y. Constitutive model of granular soils using fractional-order plastic-flow rule. *Int. J. Geomech.* 2017;17(8):04017025.
50. Yao YP, Sun DA, Luo T. A critical state model for sands dependent on stress and density. *Int. J. Numer. Anal. Methods Geomech.* 2004;28(4):323-337.
51. Yao YP, Hou W, Zhou AN. UH model: three-dimensional unified hardening model for overconsolidated clays. *Géotechnique.* 2009;59(5):451-469.
52. Gao ZW, Zhao JD. A non-coaxial critical-state model for sand accounting for fabric anisotropy and fabric evolution. *Int. J. Solids. Struct.* 2017;106-107:200-212.
53. Zhao JD, Gao ZW. Unified anisotropic elasto-plastic model for sand. *J. Eng. Mech.* 2016;142(1):04015056.
54. McDowell GR, Hau KW. A generalised Modified Cam clay model for clay and sand incorporating kinematic hardening and bounding surface plasticity. *Gran. Matter.* 2004;6(1):11-16.
55. Been K, Jefferies MG. A state parameter for sands. *Géotechnique.* 1985;35(2):99-112.
56. Li XS, Wang Y. Linear representation of steady-state line for sand. *J. Geotech. Geoenviron. Eng.* 1998;124(12):1215-1217.
57. Li XS, Dafalias YF. Dilatancy for cohesionless soils. *Géotechnique.* 2000;50(4):449-460.
58. Le TH, Dormieux L, Jeannin L, Burlion N, Barthélémy JF. Nonlinear behavior of matrix-inclusion composites under high confining pressure: application to concrete and mortar. *Comptes Rendus Mécanique.* 2008;336(8):670-676.
59. Königsberger M, Pichler B, Hellmich C. Micromechanics of ITZ-aggregate interaction in concrete part I: stress concentration. *J. Am. Ceram. Soc.* 2014;97(2):535-542.
60. Housley GT, Amorosi A, Rojas E. Elastic moduli of soils dependent on pressure: a hyperelastic formulation. *Géotechnique.* 2005;55(5):383-392.
61. Gouzarzy M, König D, Schanz T. Small strain stiffness of granular materials containing fines. *Soils Found.* 2016;56(5):756-764.
62. Gouzarzy M, König D, Schanz T. Small and intermediate strain properties of sands containing fines. *Soil Dyn. Earthq. Eng.* 2018;110:110-120.
63. Shi XS, Zhao J. Practical estimation of compression behavior of clayey/silty sands using equivalent void ratio concept. *J. Geotech. Geoenviron. Eng.* 2020;146(6):04020046.
64. Bardet JP, Choucair W. A linearized integration technique for incremental constitutive equations. *Int. J. Numer. Anal. Methods Geomech.* 1991;15(1):1-19.
65. Yagiz S. Brief note on the influence of shape and percentage of gravel on the shear strength of sand and gravel mixtures. *Bull. Eng. Geol. Environ.* 2001;60(4):321-323.
66. Zhang HY, Xu WJ, Yu YZ. Triaxial tests of soil-rock mixtures with different rock block distributions. *Soils Found.* 2016;56(1):44-56.
67. Shi XS, Liu K, Yin J. Effect of initial density, particle shape and confining stress on the critical state behavior of gap-graded soils. *J. Geotech. Geoenviron. Eng.* 2021:147.
68. Herle I, Gudehus G. Determination of parameters of a hypoplastic constitutive model from properties of grain assemblies. *Mech. Cohesive-frict. Mater.* 1999;4(5):461-486.
69. Zhang HY. *Study on Mesostructure Mechanics and Scaling Effect of Soil-Rock Mixture.* Department of Hydraulic Engineering, Tsinghua University; 2016. *Ph.D. thesis.*
70. Silva SD. Three runway system project (3RS project), contract 3206-main reclamation works. *Report for ZHECC-CCCC-CDC Joint Venture.* Hong Kong; 2016. 7076481/R00.
71. Yang ZY, Juo JL. Interpretation of sieve analysis data using the box-counting method for gravelly cobbles. *Can. Geotech. J.* 2001;38(6):1201-1212.
72. Zhao MH, Zou XJ, Zou PX. Disintegration characteristics of red sandstone and its filling methods for highway roadbed and embankment. *J. Mater. Civ. Eng.* 2007;19(5):404-410.

**How to cite this article:** Shi XS, Zhao J, Gao Y. A homogenization-based state-dependent model for gap-graded granular materials with fine-dominated structure. *Int J Numer Anal Methods Geomech.* 2021;45:1007–1028.  
<https://doi.org/10.1002/nag.3189>